

1 **Title:** Enhancing Cardiovascular Monitoring: A Non-Linear Approach to RR Interval
2 Dynamics in Exercise and Recovery.

3 **Authors:** : Matías Castillo-Aguilar^{1,2}, Diego Mabe-Castro^{1,2}, David Medina¹, Cristian
4 Núñez-Espinosa^{1,3*}.

5 ¹ Centro Asistencial Docente e Investigación (CADI-UMAG), University of Magallanes,
6 Punta Arenas, Chile.

7 ² Kinesiology Department, University of Magallanes, Punta Arenas, Chile.

8 ³ School of Medicine, University of Magallanes, Punta Arenas, Chile.

9 ****Correspondence:***

10 Cristian Núñez-Espinosa, School of Medicine, University of Magallanes, Punta Arenas,
11 Chile. Centro Asistencial de Docencia e Investigación CADI-UMAG, Chile. e-mail:
12 cristian.nunez@umag.cl. Address: Avenida Bulnes 01855, Box 113-D. Phone: +56 61
13 2201411.

Abstract

Objective: This study aims to develop and validate a novel non-linear model for characterizing RR interval (RRi) dynamics during exercise and recovery, enhancing the understanding of the cardiac autonomic function and its implications for both clinical practice and athletic training. **Methods:** A cohort of 272 participants underwent a validated exercise protocol, during which continuous heart rate data, including RR intervals, were collected. A non-linear logistic approach was employed to model the fluctuations in RRi. Sobol sensitivity analysis was conducted to assess the influence of model parameters on RR dynamics. **Results:** The proposed model successfully captured the complex fluctuations in RRi, demonstrating significant sensitivity to baseline RRi and recovery proportions, which were identified as key drivers of model output variance. Validation against physiological benchmarks confirmed the model's robustness and accuracy in real-time assessments, indicating its effectiveness in reflecting autonomic recovery post-exercise. **Conclusion:** This study presents a novel non-linear model of RR interval dynamics that provides valuable insights into cardiac autonomic responses during exercise and recovery. By enhancing the precision of cardiovascular assessments, the model holds significant promise for supporting personalized health interventions and optimizing performance in both clinical and athletic settings.

Keywords: Heart Rate Variability, Exercise Physiology, Autonomic Nervous System, Cardiovascular System, Models, Theoretical, Logistic Models.

36 **Introduction**

37 Current research has extensively examined the mechanisms underlying cardiac autonomic
38 dynamics in response to exercise and their links to health-related quality of life and
39 cardiovascular disease risk. Understanding these autonomic processes offers valuable
40 insights into optimizing exercise-induced adaptations, with implications for younger and
41 older individuals.

42 In this context, the study of R-R intervals (RRi) in response to exercise has emerged as an
43 important research area, given its relevance to cardiovascular health, athletic performance,
44 and physiological adaptation (Kristal-Boneh et al., 1995; Thayer et al., 2010; Dong, 2016;
45 Lundstrom et al., 2023). Unlike heart rate variability (HRV), which aggregates autonomic
46 responses over time, RRi analysis provides a more granular, direct view of cardiac
47 electrical activity during or immediately following exercise, particularly in older adults
48 (Mongin et al., 2022; Castillo-Aguilar et al., 2023; Mabe-Castro et al., 2024). Analyzing
49 the temporal dynamics of RRi (i.e., the time between successive heartbeats) provides
50 invaluable insights into how the cardiovascular system behaves to and recovers from
51 physical stressors such as exercise-induced fatigue and competition-related strain (Castillo-
52 Aguilar et al., 2021; Eser et al., 2022a).

53 Understanding these fluctuations is particularly relevant during dynamic exercise periods,
54 where the autonomic nervous system (ANS) shifts between parasympathetic withdrawal
55 and sympathetic activation (Boettger et al., 2010). Modeling RRi dynamics, rather than
56 relying on broader HRV metrics, allows for a direct assessment of physiological markers of
57 autonomic adaptation to stress (Hautala et al., 2003). This approach is valuable for
58 identifying recovery patterns and understanding cardiovascular reactivity across individuals
59 with various fitness levels (Mongin et al., 2022).

60 Despite its importance, modeling RRi behavior during and after exercise in a continuous
61 measurement poses significant challenges. Traditional approaches, such as linear regression
62 and time-series analysis, often fail to capture the intricate transitions in RRi, especially
63 under intense exertion and recovery phases. This difficulty arises due to the inherently non-
64 linear and non-stationary nature of HRV (Gronwald et al., 2019a). While linear models

oversimplify these dynamics, advanced non-linear approaches have been developed to address the limitations of linear analysis. However, many focus on HRV summaries rather than direct RRI modeling (Gronwald et al., 2019b).

Recent studies have begun exploring non-linear models for RRI dynamics, recognizing their potential to capture the complexity of cardiovascular response to exercise. Exponential decay models, for example, have been proposed to describe RRI recovery, while logistic functions have been used to model the gradual return to baseline after high-intensity exercise (Gronwald et al., 2019b; Molkkari et al., 2020). These models offer advantages over traditional HRV metrics by providing a more detailed understanding of the cardiovascular system's response to exercise (Wu and Poon, 2003). However, despite these advancements, few models are specifically designed to capture real-time RRI fluctuations, and even fewer consider individual variability factors such as fitness level, autonomic balance, and exercise intensity (Kanniainen et al., 2023).

Given RRI's unique characteristics, direct relationship with cardiac electrical activity, and responsiveness to autonomic changes, a model that accurately represents RRI's non-linear fluctuations during exercise and recovery is compelling. Such a model would offer a more physiologically relevant representation of the heart's behavior compared to the broader HRV indices commonly used in research (Bacopoulou et al., 2021).

Hence, the primary objective of this paper is to present a novel non-linear model that characterizes RRI fluctuations during exercise and recovery. This model is designed to capture the complex, real-time changes in RRI, providing meaningful parameters that can enhance our understanding of the physiological processes underlying cardiovascular adaptation to exercise. By focusing exclusively on RRI, the model can deliver insights directly applicable to athletic training regimens, recovery protocols, and clinical practices to improve cardiovascular health. The proposed model seeks to bridge the gap between existing modeling frameworks and the physiological reality of RRI dynamics during exercise.

92 **Methods**

93 **Model Specification**

94 The mathematical model proposed to characterize the RRI response to exercise and
95 recovery is defined by Equation 1.

$$96 \quad \text{RRI}(t) = \alpha + \frac{\beta}{1 + e^{\lambda(t-\tau)}} + \frac{-\beta \cdot c}{1 + e^{\phi(t-\tau-\delta)}} \quad (1)$$

97 This model includes two logistic functions representing the RRI dynamics across exercise
98 and recovery phases. The first logistic term models the decrease in RRI during exercise,
99 where the parameter β denotes the magnitude of this decline. The rate of decrease is
100 governed by λ , while τ represents the onset of the RRI decrease or the time the
101 physiological shift begins.

102 The second logistic term accounts for RRI recovery post-exercise. Here, c scales the
103 magnitude of recovery relative to the initial decline represented by β , effectively capturing
104 the proportion of the decline regained during recovery. The rate at which RRI returns to
105 baseline is controlled by ϕ , and δ indicates the lag following the cessation of exercise,
106 marking the beginning of recovery.

107 This logistic structure is well-suited to modeling the RRI dynamics, providing a smooth,
108 continuous transition for the decline and recovery phases. Logistic growth functions are
109 particularly effective in physiological modeling contexts, where transitions (e.g., rest to
110 exercise or exercise to recovery) occur gradually and non-linearly. Compared to conditional
111 models, which may introduce abrupt transitions, this model is designed to minimize
112 discontinuities, thus offering a realistic representation of RRI responses without artifacts.

113 **Sensitivity to model parameters**

114 To assess the sensitivity of model parameters in influencing RRI over time, we
115 implemented a Sobol sensitivity analysis using Monte Carlo simulations. Sobol analysis
116 was selected for its robustness in handling non-linear and non-monotonic relationships,
117 which are intrinsic to RRI dynamics in response to exercise. To compute Sobol indices,

1000 Monte Carlo simulations were conducted, each involving 1000 randomly sampled parameter sets (1,000,000 model runs in total). For each set of parameters, RR_i were calculated at each time point t across a range from 0 to 20 minutes at intervals of 0.1 minutes (i.e., 6 seconds). The resulting Sobol indices provided a measure of the contribution of each parameter to the variance in RR_i at each time point.

The first-order Sobol index for each parameter was computed by isolating the variance attributable to each parameter while averaging over the others. To achieve this, we perturbed each parameter individually while holding all other parameters at their average values across the samples. The proportion of variance explained by each parameter at each time point was calculated by dividing the variance of the estimated RR_i of the perturbed parameter by the total variance, which accounts for the variation in all model parameters simultaneously, yielding time-dependent Sobol indices. The selected parameter ranges, provided in Table 1, reflect a 50% variation in both directions from a reference value for each parameter.

	α	β	c	λ	ϕ	τ	δ
x 0.5	400	-200	0.5	-1.151	-0.602	2.5	1
Reference	800	-400	1.0	-2.303	-1.203	5	2
x 1.5	1200	-600	1.5	-3.454	-1.806	7.5	3

Table 1. Parameter ranges for sensitivity analysis to be used as the limits to sample from uniform distribution and designed to evaluate model response to variability. Each parameter's range reflects a $\pm 50\%$ variation from its reference value. It is worth noting that reference values for λ and ϕ parameters were set considering a reference rate of 90% and 70% change per minute in the original scale of these parameters.

Sobol sensitivity analysis was selected due to its robustness in decomposing the variance attributed to each parameter in complex, non-linear, and non-monotonic models, such as the present logistic model of RR_i . While methods like the Morris screening technique offer computational efficiency, Sobol's approach provides a more comprehensive assessment of parameter interactions, making it particularly suitable for physiological models where interaction effects may be critical to interpret.

Usage of real-world RRI data

To further assess the performance and applicability of the proposed model, real-world RRI data were analyzed in addition to the synthetic data generated through simulation. This dataset was derived from a cohort participating in the FONDECYT Project No. 11220116, funded by the Chilean National Association of Research and Development (ANID). Ethical approval was granted by the Ethics Committee of the University of Chile (ACTA No. 029-18/05/2022) and the Ethics Committee of the University of Magallanes (No. 008/SH/2022).

The dataset consisted of 272 participants who underwent a validated exercise protocol encompassing rest, exercise, and recovery phases within a single, continuous measurement session (Castillo-Aguilar et al., 2023). Continuous heart rate data, including RRI, were collected using the Polar Team2 system (Polar®) application, capable of capturing dynamic fluctuations associated with varying exercise intensities and recovery.

Preprocessing steps were conducted to remove artifacts and ectopic heartbeats, with less than 3% of data excluded following established guidelines (Malik, 1996). The preprocessed RRI data were then aggregated into time intervals to facilitate analysis, allowing the examination of acute exercise responses and post-exercise recovery patterns.

This real-world dataset provided a critical context for validating the model's predictive capability against observed physiological responses, offering a robust foundation for understanding RRI dynamics under physical activity conditions.

Parameter Estimation

Parameter estimation was performed using Hamiltonian Monte Carlo (HMC) with the No-U-Turn Sampler (NUTS) to explore the parameter space. This method suits high-dimensional spaces and utilizes gradient information for efficient sampling. The parameters α , β , c , λ , ϕ , τ , and δ were estimated by sampling from the posterior distribution, which was constructed from observed RRI data and model predictions. The Bayesian framework allows the incorporation of prior distributions for parameters, enhancing the reliability of the estimates.

The gradient of the log-likelihood function for each parameter was computed during estimation using the brms R package, which employs the Stan probabilistic programming language. Convergence of the HMC chains was assessed using standard diagnostics, including R-hat values, which were kept below 1.01 for all parameters, and effective sample sizes, which were targeted at a minimum of 1,000 for each parameter. Trace plots were inspected to confirm stable mixing, and potential issues with autocorrelation were addressed by increasing the warm-up period to ensure chain independence. These diagnostics collectively confirmed reliable posterior estimates for each parameter.

The fitting process utilized five Markov Chain Monte Carlo (MCMC) chains, each consisting of 10,000 iterations with a burn-in period of 5,000 iterations, resulting in 25,000 post-warmup samples.

To enhance the exploration of parameter space, we performed a two-stage analysis: individual-level and group-level estimates.

Individual-level analysis

Firstly, each subject's RRI data $RRi_{i,t}$ was standardized against his mean $R\bar{R}i_t$ and standard deviation σ_{RRi_t} to improve convergence and exploration of the posterior distribution. The standardized RRI data $y_{i,t}$ for each time point t was computed as:

$$y_{i,t} = \frac{RRi_{i,t} - R\bar{R}i_t}{\sigma_{RRi_t}}$$

This standardization allowed the model to focus on relative changes in RRI dynamics, independent of individual baseline differences.

The model for each subject i was then specified in terms of standardized RRI data $y_{i,t}$:

$$y_{i,t} = \alpha_i + \frac{\beta_i}{1 + e^{\lambda_i \cdot (t - \tau_i)}} + \frac{-\beta_i \cdot c}{1 + e^{\phi_i \cdot (t - \tau_i - \delta_i)}} + \epsilon_{i,t}$$

where α_i , β_i , c_i , λ_i , ϕ_i , τ_i , δ_i are the individual-specific model parameters and $\epsilon_{i,t} \sim \mathcal{N}(0, \sigma^2)$ is the residual error term at each time point t .

194 Afterwards, we transformed the estimated α and β parameters back to the original RRI
 195 scale, ensuring a physiologically meaningful interpretation. The transformation for each
 196 subject i is given by:

$$\begin{aligned} \alpha_i^{\text{RRI}} &= \alpha_i \cdot \sigma_{\text{RRI}_i} + \bar{\text{RRI}}_i \\ \beta_i^{\text{RRI}} &= \beta_i \cdot \sigma_{\text{RRI}_i} \end{aligned}$$

198 Priors were chosen based on physiological constraints and graphical visualization of
 199 standardized RRI data, ensuring identifiability of model parameters by constraining the
 200 parameter space to plausible values, which improves model convergence. The prior
 201 distributions are defined as follows:

$$\begin{aligned} \alpha &\sim \mathcal{N}(1, 0.5) \\ \beta &\sim \mathcal{N}(-2.5, 0.5) \text{ with } \beta \leq 0 \\ c &\sim \mathcal{N}(0.8, 0.2) \text{ with } c \geq 0 \\ \lambda &\sim \mathcal{N}(-2, 0.5) \text{ with } \lambda \leq 0 \\ \phi &\sim \mathcal{N}(-2, 0.5) \text{ with } \phi \leq 0 \\ \tau &\sim \mathcal{N}(5, 0.5) \text{ with } \tau \geq 0 \\ \delta &\sim \mathcal{N}(5, 0.5) \text{ with } \delta \geq 0 \end{aligned}$$

203 Simulated standardized RRI dynamics based on prior parameter distributions are shown in
 204 Figure 1.

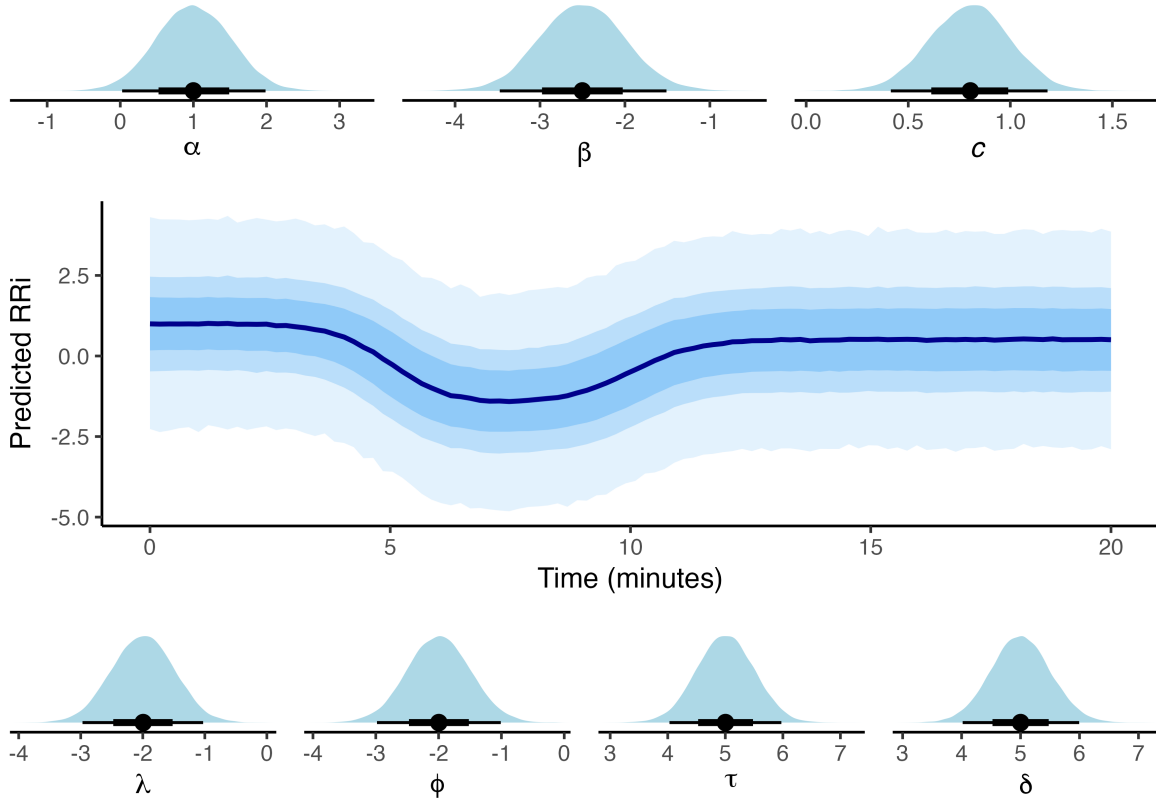


Figure 1. Simulated standardized RRI dynamics based on prior parameter distributions, depicting predicted RRI responses to exercise. Shaded areas represent 95%, 80%, and 60% quantile credible intervals, offering insight into expected physiological variability across parameters.

Group-level analysis

After obtaining the posterior distribution for each subject's parameters, each parameter's mean (θ^{obs}) and standard error (ϵ) were calculated. These estimates were then used as input data to create a univariate hierarchical model, capturing variability at both the subject and group levels. The model is described as follows:

For each subject i , we estimated an interdependent stochastic process in which the true parameter $\theta_{k,i}$, with $k \in \{\alpha, \beta, c, \lambda, \phi, \tau, \delta\}$ with their corresponding standard error $\epsilon_{k,i}$ was used to model the observed parameter $\hat{\theta}_{k,i}$ as:

$$\theta_{k,i}^{\text{obs}} \sim \mathcal{N}(\theta_{k,i}, \epsilon_{k,i})$$

219 Then, the true parameter $\theta_{k,i}$ was further modeled as:

220
$$\theta_{k,i} \sim \mathcal{N}(\mu_k + b_{k,i}, \sigma_k^2)$$

221 where μ_k is the group-level mean for parameter k , $b_{k,i}$ represents the subject-level random
222 effect for subject i on parameter k and σ_k^2 is the residual variance for parameter k . The
223 subject-level effects $b_{k,i}$ were assumed to be distributed as $b_{k,i} \sim \mathcal{N}(0, \sigma^2)$, with σ being
224 the standard error of the subject-level effect.

225 This hierarchical structure enables us to capture individual variability through subject-level
226 random effects while estimating group-level effects across all parameters, thus providing
227 estimates into subject and population-level model parameters.

228 **Model Evaluation**

229 The primary performance metrics included R^2 , root mean square error (RMSE) and mean
230 absolute percentage error (MAPE), estimated for each subject. Bootstrap resampling across
231 each metric was performed to estimate the mean performance of the model. These metrics
232 were selected for their capacity to assess model capacity to predict the observed RRI and to
233 quantify absolute and relative errors, thereby providing a comprehensive assessment across
234 the varying scales of RRI dynamics, including resting baseline, peak decline, and recovery.

235 Also, residual analysis was conducted to evaluate the model's accuracy in capturing RRI
236 dynamics. Residuals were defined as the difference between observed and predicted RRI
237 values. These residuals were analyzed for temporal structure and partial autocorrelation to
238 ensure that no systematic patterns remained in the errors. This indicates that the model has
239 sufficiently captured the underlying dynamics of the RRI response to exercise.

Results

Non-linear model and deterministic behaviour

RRi as a linear combination of logistic functions

According to the proposed model in Equation 1, the dynamics of RRi in response to physical exertion can be represented as a linear combination of a baseline RRi α and two logistic functions denoted as $f_1(t)$ and $f_2(t)$. The function $f_1(t)$ models the initial decay in RRi following the initiation of exercise while $f_2(t)$ characterizes the recovery phase after exercise cessation.

The fundamental structure of both logistic functions can be expressed as:

$$f(t) = \frac{a_1}{1 + e^{a_2(t-a_3)}} \quad (2)$$

In this equation, a_1 represents the asymptotic value approached by the logistic function, which can be either positive (indicating an increase) or negative (indicating a decrease). For $f_1(t)$, this parameter is specified as β , indicating the absolute change in RRi at the onset of exercise. In contrast, for $f_2(t)$, a_1 is reparameterized as $-\beta \cdot c$, where c denotes the proportion of change relative to the initial drop indicated by β . This reparameterization ensures that, after the initial decline, the second logistic function facilitates the return of RRi toward the baseline value α .

The parameter a_2 defines the rate at which the specified increase or decrease occurs. This rate parameter is expressed on a logarithmic scale; to convert it to a percentage change per unit of time, it can be scaled as $1 - \exp(a_2)$. For instance, a 90% decrease per unit time corresponds to $a_2 = \log(1 - 0.9)$, resulting in an approximate value of -2.302585.

The parameter a_3 serves as an activation threshold, causing the value within the exponential function, and consequently, the value in the denominator, to increase significantly until reaching a_3 . Beyond this point, the denominator approaches 1, allowing the logistic function to attain the asymptotic level determined by the numerator. Figure 2 illustrates the behavior of the model constituents.

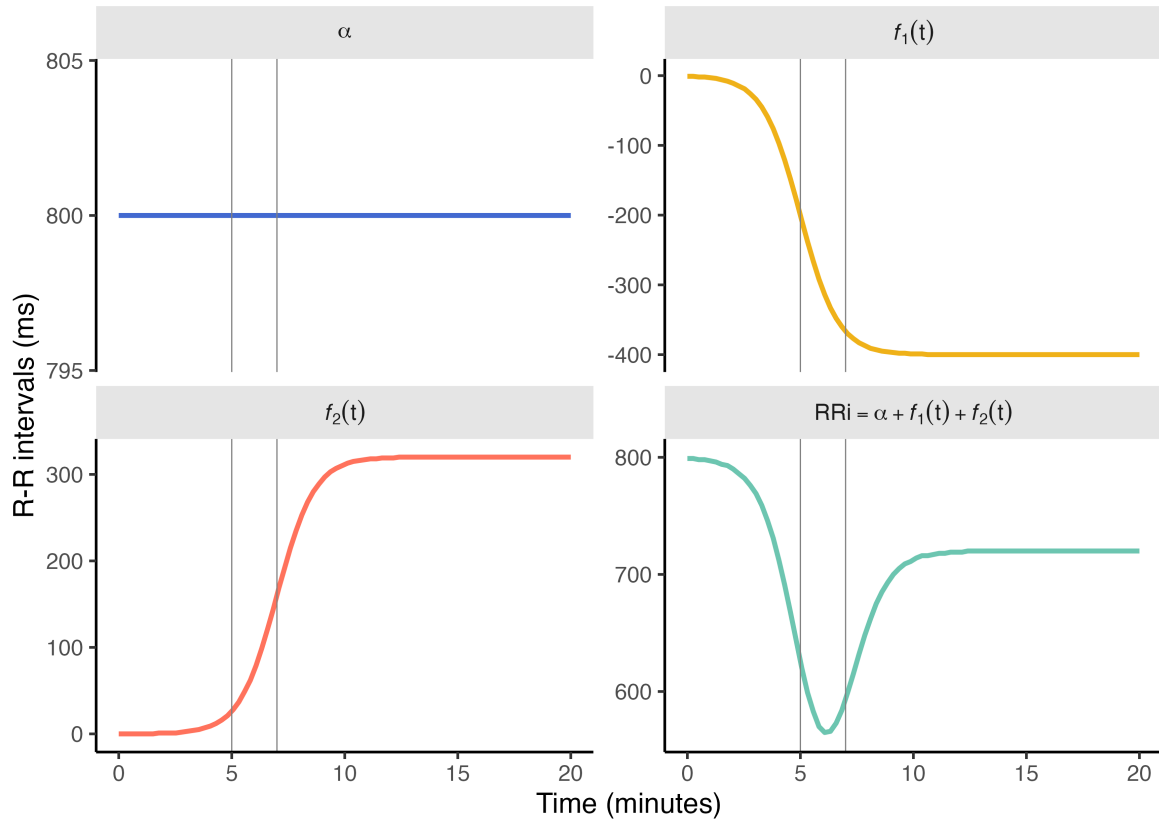


Figure 2. The RRI dynamics in response to exercise are expressed as a linear combination of model constituents based on the baseline RRI α and two logistic functions, denoted $f_1(t)$ and $f_2(t)$, respectively.

Sensitivity to parameter variability

Sobol sensitivity analysis reveals that the parameter α exerts the most substantial influence on the model's output, followed by parameters c and δ . In contrast, parameters β , λ , and ϕ demonstrate relatively minor effects, with some values crossing zero, indicating negligible influence within the tested parameter ranges.

Individual perturbation of each parameter highlighted that RRI dynamics are sensitive to the baseline RRI parameter, α . Conversely, the rate parameters for the initial decay during exercise, λ , and the recovery post-exercise, ϕ , show lower sensitivity, suggesting that they are not primary sources of variation in predicted RRI trajectories when assessed in isolation. The results of the sensitivity analysis are illustrated in Figure 3.

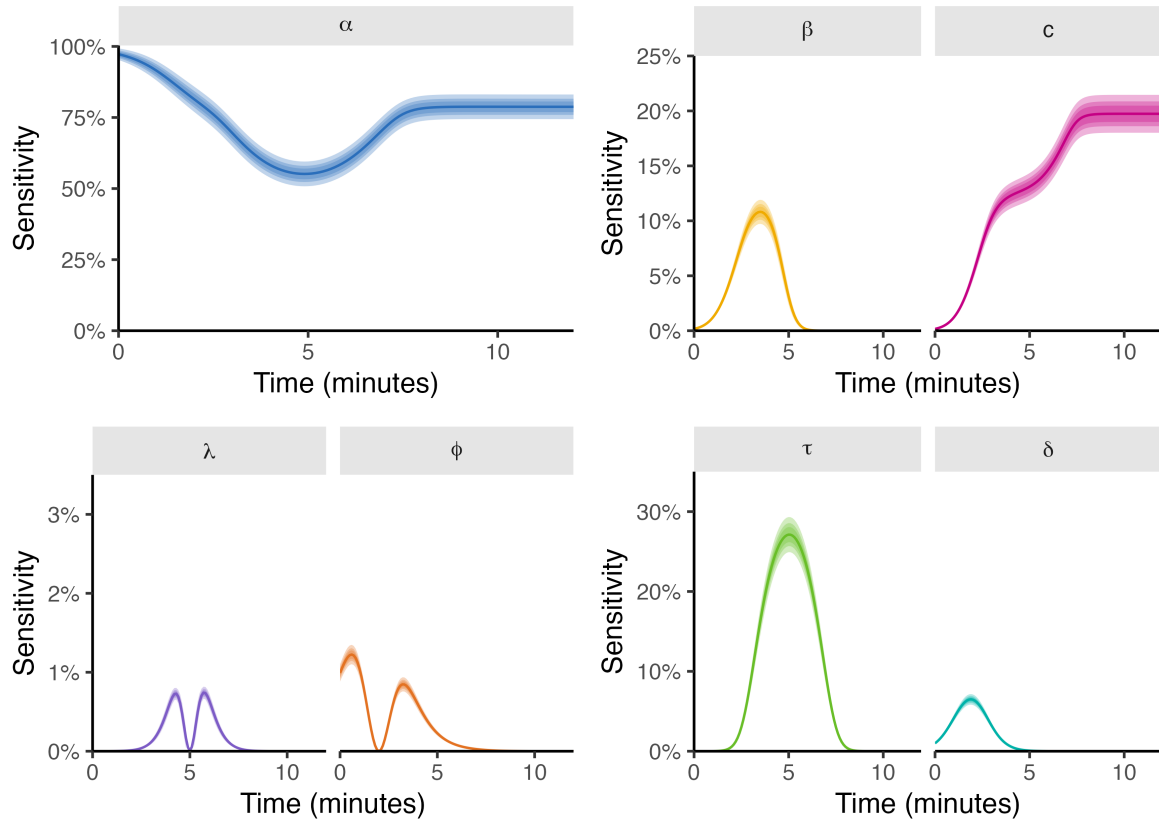


Figure 3. Sensitivity analysis results illustrate the impact of parameter variability on model predictions and the percentage of explained variance accounted for each model parameter. Shaded areas represent 95%, 80%, and 60% CI estimated from Monte Carlo samples. Time in the x-axis is truncated at 12 minutes, given that around this time, the proportion of the total variance explained by the respective model parameter stabilizes respective of time.

Despite the limited sensitivity of λ and ϕ to mean RRi, these parameters play a pivotal role in determining the rate of change in RRi in response to physical exertion. Therefore, they can significantly affect RRi dynamics over time. Figure 4 depicts the influence of these rate parameters on RRi fluctuations over time.

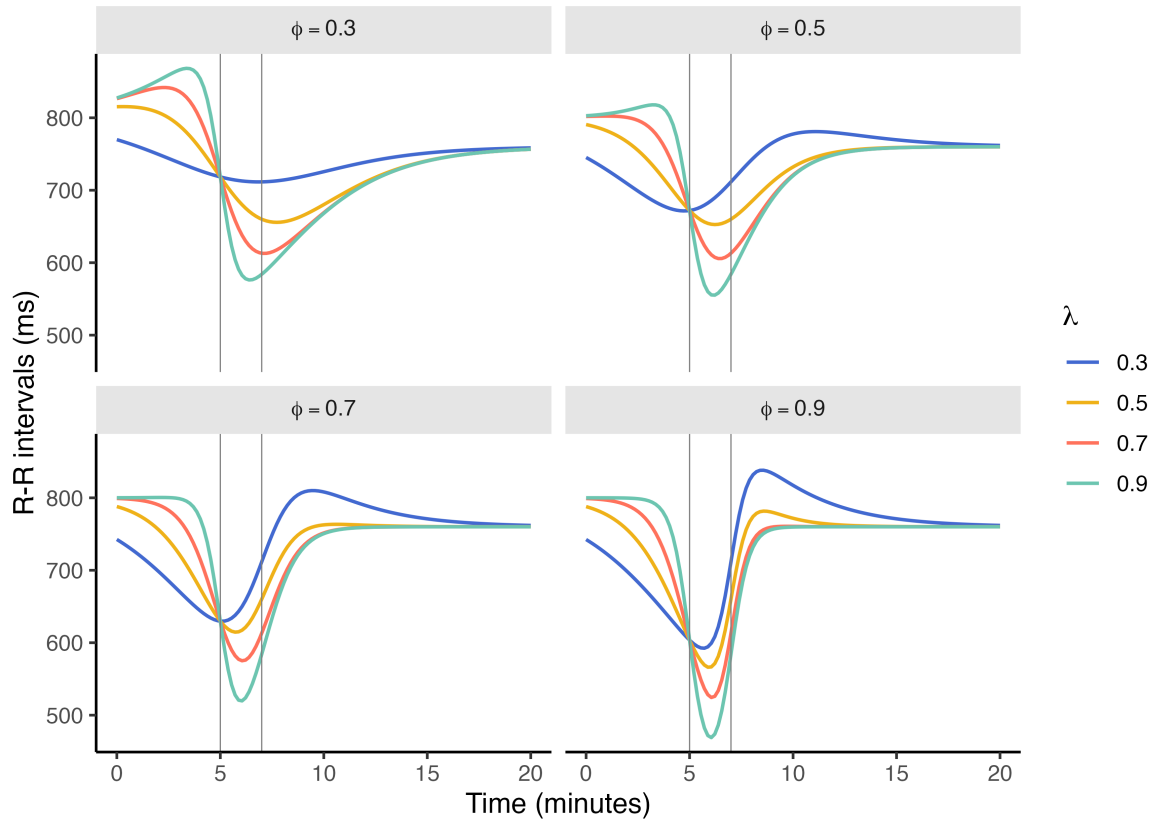


Figure 4. Simulated RRi dynamics during exercise with varying λ and ϕ rate parameters expressed as percent change per unit of time. In this simulation, the exercise-induced RRi drop occurs at 5 minutes (τ), and cardiovascular recovery begins 2 minutes after exercise initiation (δ). The model assumes a 90% recovery ($c = 0.90$) of RRi values following a 400 ms drop (β) from a baseline of 800 ms (α).

Model behavior to real RRi data

Sample characteristics

The sample used to assess RRi dynamics consists of a group of 272 subjects selected from a local community of elderly individuals. The sample characteristics can be seen in Table 2

Characteristic	Overall	Female	Male
Sex	—	217 (79.8%)	55 (20.2%)
Age	71.14 ± 6.03	70.73 ± 6.27	72.73 ± 4.7
SBP (mm hg)	130.23 ± 17.07	129.58 ± 17.37	132.8 ± 15.69
DBP (mm hg)	77.1 ± 9.58	76.68 ± 9.83	78.75 ± 8.4

Characteristic	Overall	Female	Male
MAP (mm hg)	94.81 \pm 10.69	94.31 \pm 10.95	96.76 \pm 9.45
PP (mm hg)	53.14 \pm 14.07	52.9 \pm 14.26	54.05 \pm 13.38
BMI	30.66 \pm 5.43	30.7 \pm 5.64	30.53 \pm 4.53
Weight (kg)	75.06 \pm 14.23	73.88 \pm 14.09	79.69 \pm 13.95
Height (cm)	156.56 \pm 9.18	155.29 \pm 8.46	161.55 \pm 10.24

Table 2. Sample characteristics from which, continuous RRI monitoring data was collected during a rest-exercise-rest protocol. Data is presented as Mean \pm SD.

Initial exploration of RRI dynamics using two-dimensional density kernel estimation (see Figure 5) indicates a clear drop in RRI around the 5-7 minutes mark, associated the exercise-induced cardiovascular stress. However, greater variability across individuals in post-exercise recovery can be observed.

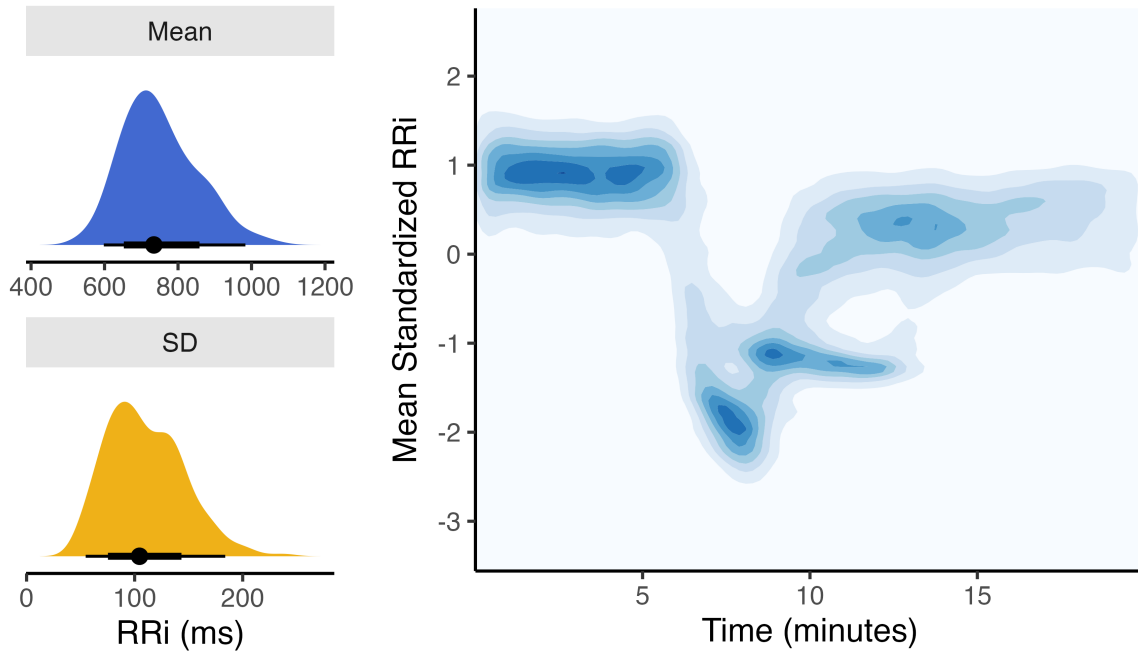


Figure 5. Left panel shows the mean and standard deviation (SD) from each of the subject's RRI recordings, used for the standardization process. Right panel indicates the 2D kernel density of standardized RRI dynamics over time from a sample of individuals subjected to the rest-exercise-rest protocol. Darker colors indicate greater probability density. The contrary can be said about lighter colors.

Model performance

Relative performance metrics, estimated through bootstrapped resampling, suggest that the model tends to deviate a 3.4% (CI_{95%}[3.06, 3.81]) from the observed RRI data. This is equivalent to a 32.6 ms in the RRI scale (CI_{95%}[30.01, 35.77]). Residuals analysis showed that the estimated partial correlation function (ACF) from the model residuals indicates a correlation among non-explained errors greater than 0.1 up to the 5th lag. However, the partial ACF is significant (CI-wise) and strictly positive or negative up to the second lag. Correlations among model residuals against other time indices remained insignificant (see Figure 6).

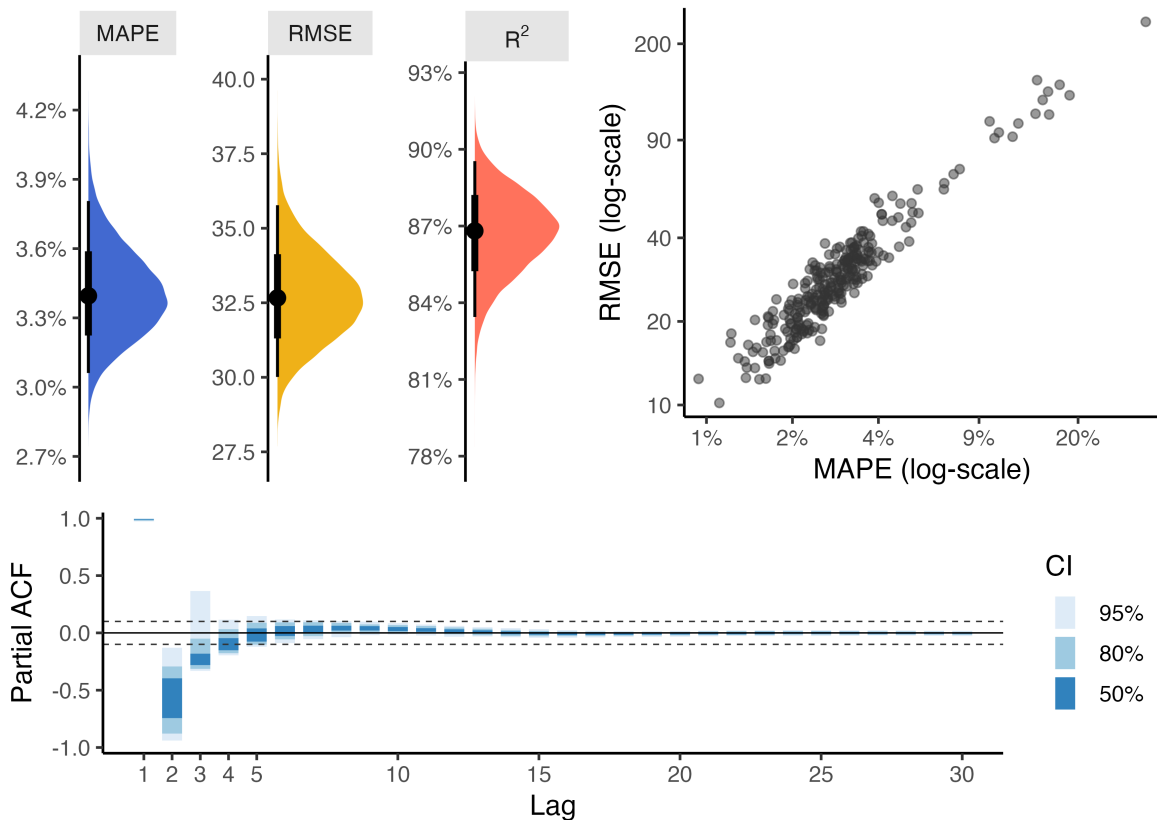


Figure 6. Individual-level performance metrics. Left upper panels indicates bootstrapped MAPE and RMSE, as metrics of relative and absolute model deviance from observed RRI. Upper right panel shows the individual-level estimates of model performance and the relationship between them. Lower panel indicates the partial autocorrelation function (ACF) of model residuals with corresponding quantile-based CI.

327 *Group-level estimates*

328 Once subject-level RRi data was fitted using the proposed non-linear equation, a
329 population-parameter value was estimated with a generalized hierarchical model with
330 measurement error as part of an interdependent stochastic process using the mean and
331 standard error of the estimated posterior distribution of the subject-level parameter, derived
332 from HMC-NUTS.

333 The *alpha* parameter, associated with the baseline RRi before exercise, was estimated at
334 861.8 ms CI_{95%}[850.6, 872.9]. The *beta* parameter, which indicates exercise-induced drop
335 in RRi, was estimated at -345.5 ms CI_{95%}[-359.8, -331.0]. The proportion of recovery *c*,
336 which can be expressed as the magnitude relative to *beta* after exercise cessation, was
337 estimated at 0.84 CI_{95%}[0.823, 0.856].

338 The rate parameters λ and ϕ , associated with the velocity of RRi drop and recovery, were
339 estimated at -3.05 CI_{95%}[-3.16, -2.94] and -2.60 CI_{95%}[-2.71, -2.48], and after transforming
340 them into a percentage of decay per minute using $1 - \exp(\theta)$, we estimated the rate of
341 decay and recovery are 95.2% ms per minute CI_{95%}[0.947, 0.957] and 92.5% ms per minute
342 CI_{95%}[0.917, 0.933].

343 The parameters associated with the time at which the initial RRi decay occurs τ were
344 estimated at 6.71 minutes CI_{95%}[6.61, 6.81], meanwhile the time duration associated with
345 the exercise-induced stress in RRi δ was estimated at 3.24 minutes CI_{95%}[3.05, 3.44].

346 Finally, the standard deviation around the estimated RRi data σ , associated with the non-
347 modeled noise, was estimated at 27.6 ms CI_{95%}[26.5, 28.7]. In Figure 7, the model
348 parameter's posterior distribution can be observed.

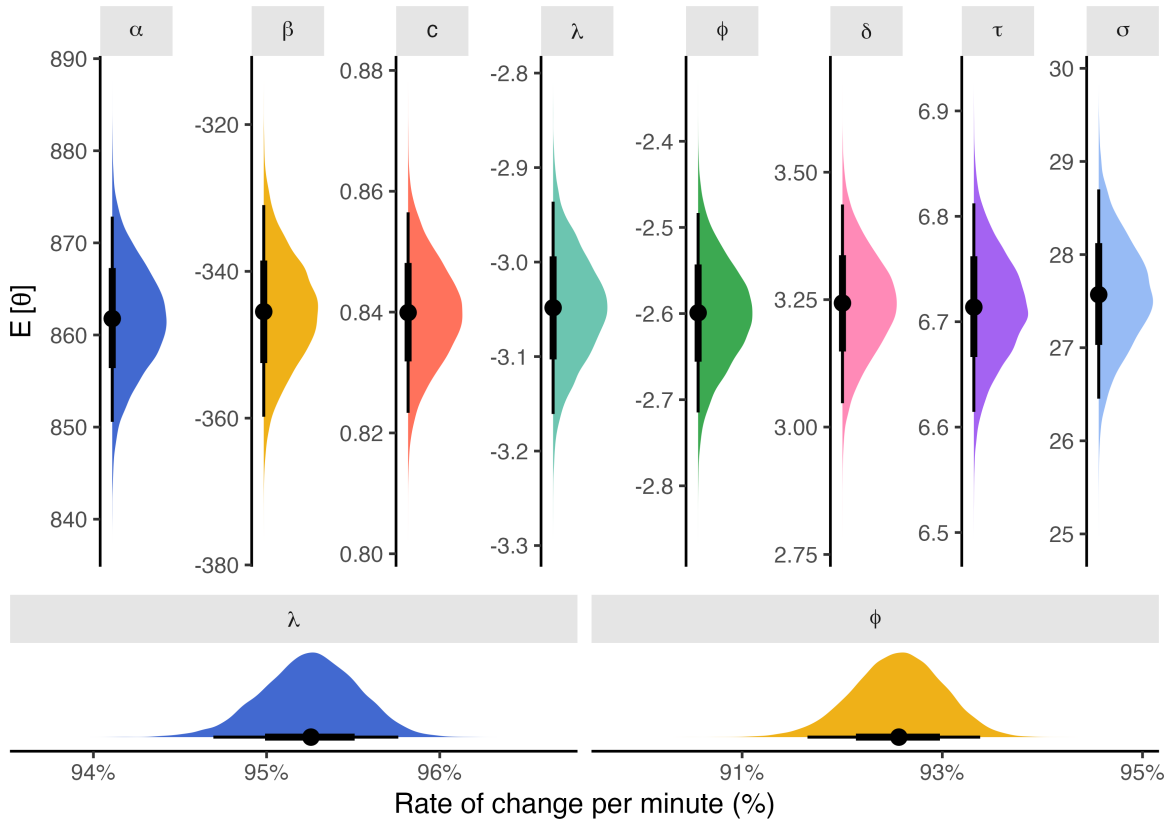


Figure 7. Posterior probability distributions from group-level estimates of the expectation of each model parameter ($E[\theta]$) with quantile-based 95% CI (upper panel), and the transformed rate parameters into a percentage scale (lower panel).

Discussion

This study presents a non-linear model designed for RRI fluctuations during exercise and recovery, providing an in-depth view of cardiac autonomic dynamics. By focusing on RRI rather than aggregate HRV metrics, our approach enables real-time tracking of cardiovascular responses to physical stress, which has implications for clinical and athletic applications. This model marks a step forward in computational physiology, bridging the gap between theoretical frameworks and practical monitoring applications.

The Sobol sensitivity analysis revealed baseline RRI (α) and recovery proportion (c) as key drivers of model output variance that are consistent with physiological expectations. Baseline RRI reflects intrinsic cardiac properties, while recovery proportion captures

autonomic re-engagement post-exercise, central to cardiovascular adaptation (Hautala et al., 2003). The relatively low sensitivity of decay and recovery rate parameters (λ and ϕ) suggests the model is robust to moderate fluctuations in these rates, enhancing its reliability for both individualized and group-based applications.

Compared to previous research, our findings align with the importance of capturing nonlinear dynamics in heart rate variability to understand cardiac responses during exercise (Gronwald et al., 2019a). Similarly, previous studies have shown that dynamic fluctuations in RRi can serve as critical indicators of cardiorespiratory fitness, supporting the need for models to address the complexity of cardiovascular responses during physical stress (Mongin et al., 2022). However, while many existing models focus primarily on linear metrics or aggregate HRV measures, our study provides a high-resolution analysis of RRi dynamics that enhances interpretability and application across diverse fitness levels and exercise intensities.

Sobol analysis was selected for its capacity to handle non-linear, time-varying relationships, but it assumes parameter independence and demands substantial computational resources (Herman et al., 2013; Cheng et al., 2017; Harenberg et al., 2017). This assumption may overlook interdependencies typical in biological systems, where parameters such as decay rates and recovery kinetics often interact. For future work, alternative sensitivity methods, such as Bayesian sensitivity analysis, could address interdependencies and improve interpretive accuracy in complex biological contexts. Additionally, real-time applications in resource-limited environments may benefit from computational optimizations, such as surrogate modeling or sparse-grid approximations, to reduce processing time while maintaining analytical depth (Bornn et al., 2010; Xue and Zaidi, 2021).

The practical application of this model extends to clinical monitoring and athletic training, but further validation is essential to confirm its robustness in real-world conditions. To support clinical decision-making, future studies should validate the model against established physiological benchmarks, such as VO_2 max and lactate thresholds, facilitating its integration into routine health assessments. For instance, this model could be valuable in cardiovascular rehabilitation programs, where tracking real-time autonomic responses can

help personalize exercise regimens, ensuring adequate recovery without overstressing the cardiovascular system. Furthermore, for at-risk populations, the model could assist in detecting autonomic irregularities indicative of early cardiovascular dysfunction (Thayer et al., 2010).

For athletic applications, the model has the potential to guide interval training, where it could help identify optimal recovery points between intense exercise bouts. This is particularly relevant given the findings of other research, which suggest that precise monitoring of heart rate dynamics can prevent overtraining and optimize performance (Eser et al., 2022b). However, extending this model beyond controlled, single-bout settings requires further validation, particularly in dynamic environments where external factors like temperature, altitude, and psychological stress can influence RRI. Integrating the model with wearable devices capable of accurately capturing RRI is essential for field applications, enabling real-time monitoring and feedback (Lundstrom et al., 2023).

Traditional models of RRI often rely on linear assumptions or simple exponential functions, which fail to capture the transient, non-stationary nature of RRI during exercise and recovery. Using logistic functions to model the decay and recovery phases, our non-linear approach accommodates gradual autonomic shifts more effectively than exponential functions, offering a physiologically relevant representation of RRI dynamics. While recent studies have developed non-linear models, many focus on HRV aggregates that summarize rather than directly model RRI changes (Molkkari et al., 2020). By concentrating on RRI, our approach offers a high-resolution view of cardiac adaptation, making it particularly valuable for clinical and athletic contexts. Adapting model parameters to real-time changes in RRI enhances sensitivity in detecting subtle shifts in autonomic state, which aggregated HRV indices may obscure (Mabe-Castro et al., 2024).

This model has limitations that warrant careful consideration. First, the uniform parameter sampling used in sensitivity analysis, though practical, may not fully capture individual variability in populations with extreme autonomic profiles or chronic health conditions. Incorporating empirical distributions or Bayesian priors based on population data could refine parameter estimates, enhancing individualization for diverse clinical populations, such as older adults or individuals with cardiovascular disease (Kristal-Boneh et al., 1995).

Moreover, an area for future research includes multi-session modeling to account for cumulative adaptations over repeated exercise sessions. Studies have shown that cumulative effects from multiple exercise bouts can introduce autonomic fatigue or adaptation (Castillo-Aguilar et al., 2021). Extending the model to track such longitudinal effects could help identify early signs of overtraining or autonomic exhaustion, providing a preventive tool for clinical and athletic populations. Additionally, considering environmental and psychological factors (i.e., such as temperature, stress, or sleep quality) would add robustness, ensuring that model predictions remain accurate across varied real-world contexts.

Conclusion

This study presents a novel non-linear model for characterizing RRi dynamics during exercise and recovery, providing a more accurate and nuanced understanding of cardiac autonomic function compared to traditional HRV metrics. Our findings emphasize the important roles of baseline RRi and recovery proportion in reflecting autonomic re-engagement, enhancing the sensitivity of real-time assessments of cardiovascular responses to physical stress. This model advances computational physiology and holds significant promise for improving cardiovascular health monitoring and performance optimization.

Authors' Contributions

Conceptualization, MC-A; Data curation, MC-A; Investigation, MC-A; Methodology, MC-A, NMD; Supervision, CN-E; Formal analysis, MC-A; Visualization, MC-A; Writing—original draft, MC-A, CN-E, [...]; Writing—review & editing, MC-A, CN-E, [...]. All authors have read and agreed to the published version of the manuscript.

Funding

This work was funded by ANID Proyecto Fondecyt Iniciación N°11220116.

Data Availability Statement

The data supporting the conclusions of this article will be available from the authors without reservation.

Conflict of Interest

The authors declare that this research was conducted without any commercial or financial relationships that could be construed as potential conflicts of interest.

References

- Bacopoulou, F., Chryssanthopoulos, S., Koutelekos, J., Lambrou, G. I., and Cokkinos, D. (2021). Entropy in cardiac autonomic nervous system of adolescents with general learning disabilities or dyslexia., in *GeNeDis 2020: Genetics and neurodegenerative diseases*, (Springer), 121–129.
- Boettger, S., Puta, C., Yeragani, V. K., Donath, L., Mueller, H.-J., Gabriel, H. H., et al. (2010). Heart rate variability, QT variability, and electrodermal activity during exercise. *Med sci sports exerc* 42, 443–8.
- Bornn, L., Doucet, A., and Gottardo, R. (2010). An efficient computational approach for prior sensitivity analysis and cross-validation. *Canadian Journal of Statistics* 38, 47–64.
- Castillo-Aguilar, M., Mabe Castro, M., Mabe Castro, D., Valdés-Badilla, P., Herrera-Valenzuela, T., Guzmán-Muñoz, E., et al. (2023). Validity and reliability of short-term heart rate variability parameters in older people in response to physical exercise. *International Journal of Environmental Research and Public Health* 20, 4456.
- Castillo-Aguilar, M., Valdés-Badilla, P., Herrera-Valenzuela, T., Guzmán-Muñoz, E., Delgado-Floody, P., Andrade, D. C., et al. (2021). Cardiac autonomic modulation in response to muscle fatigue and sex differences during consecutive competition periods in young swimmers: A longitudinal study. *Frontiers in Physiology* 12, 769085.

471 Cheng, K., Lu, Z., Wei, Y., Shi, Y., and Zhou, Y. (2017). Mixed kernel function support
 472 vector regression for global sensitivity analysis. *Mechanical Systems and Signal Processing*
 473 96, 201–214.

474 Dong, J.-G. (2016). The role of heart rate variability in sports physiology. *Experimental*
 475 *and therapeutic medicine* 11, 1531–1536.

476 Eser, P., Jaeger, E., Marcin, T., Herzig, D., Trachsel, L. D., and Wilhelm, M. (2022a).
 477 Acute and chronic effects of high-intensity interval and moderate-intensity continuous
 478 exercise on heart rate and its variability after recent myocardial infarction: A randomized
 479 controlled trial. *Annals of Physical and Rehabilitation Medicine* 65, 101444.

480 Eser, P., Jaeger, E., Marcin, T., Herzig, D., Trachsel, L., and Wilhelm, M. (2022b). Acute
 481 and chronic effects of high-intensity interval and moderate-intensity continuous exercise on
 482 heart rate and its variability after recent myocardial infarction: A randomized controlled
 483 trial. *Annals of physical and rehabilitation medicine* 65, 101444.

484 Gronwald, T., Hoos, O., and Hottenrott, K. (2019a). Effects of a short-term cycling interval
 485 session and active recovery on non-linear dynamics of cardiac autonomic activity in
 486 endurance trained cyclists. *Journal of clinical medicine* 8, 194.

487 Gronwald, T., Hoos, O., Ludyga, S., and Hottenrott, K. (2019b). Non-linear dynamics of
 488 heart rate variability during incremental cycling exercise. *Research in Sports Medicine* 27,
 489 88–98.

490 Harenberg, D., Marelli, S., Sudret, B., and Winschel, V. (2017). Uncertainty quantification
 491 and global sensitivity analysis for economic models. *Available at SSRN 2903994*.

492 Hautala, A. J., Mäkikallio, T. H., Seppänen, T., Huikuri, H. V., and Tulppo, M. P. (2003).
 493 Short-term correlation properties of r–r interval dynamics at different exercise intensity
 494 levels. *Clinical physiology and functional imaging* 23, 215–223.

495 Herman, J. D., Kollat, J. B., Reed, P. M., and Wagener, T. (2013). Method of morris
 496 effectively reduces the computational demands of global sensitivity analysis for distributed
 497 watershed models. *Hydrology and Earth System Sciences* 17, 2893–2903.

498 Kanniainen, M., Pukkila, T., Kuisma, J., Molkari, M., Lajunen, K., and Räsänen, E.
 499 (2023). Estimation of physiological exercise thresholds based on dynamical correlation
 500 properties of heart rate variability. *Frontiers in physiology* 14, 1299104.

501 Kristal-Boneh, E., Raifel, M., Froom, P., and Ribak, J. (1995). Heart rate variability in
 502 health and disease. *Scandinavian journal of work, environment & health*, 85–95.

503 Lundstrom, C. J., Foreman, N. A., and Biltz, G. (2023). Practices and applications of heart
 504 rate variability monitoring in endurance athletes. *International journal of sports medicine*
 505 44, 9–19.

506 Mabe-Castro, D., Castillo-Aguilar, M., Mabe-Castro, M., Muñoz, R. M., Basualto-Alarcón,
 507 C., and Nuñez-Espinosa, C. A. (2024). Associations between physical fitness, body
 508 composition, and heart rate variability during exercise in older people: Exploring mediating
 509 factors. *PeerJ* 12, e18061.

510 Malik, M. (1996). Heart rate variability: Standards of measurement, physiological
 511 interpretation, and clinical use: Task force of the european society of cardiology and the
 512 north american society for pacing and electrophysiology. *Annals of Noninvasive*
 513 *Electrocardiology* 1, 151–181.

514 Molkari, M., Solanpää, J., and Räsänen, E. (2020). Online tool for dynamical heart rate
 515 variability analysis., in *2020 computing in cardiology*, (IEEE), 1–4.

516 Mongin, D., Chabert, C., Extremera, M. G., Hue, O., Courvoisier, D. S., Carpena, P., et al.
 517 (2022). Decrease of heart rate variability during exercise: An index of cardiorespiratory
 518 fitness. *PLoS ONE* 17, e0273981.

519 Thayer, J. F., Yamamoto, S. S., and Brosschot, J. F. (2010). The relationship of autonomic
 520 imbalance, heart rate variability and cardiovascular disease risk factors. *International*
 521 *journal of cardiology* 141, 122–131.

522 Wu, G., and Poon, C.-S. (2003). Nonlinear neurodynamics model of heart rate variability,
 523 multifractality and chaos., in *Proceedings of the 25th annual international conference of*

524 *the IEEE engineering in medicine and biology society (IEEE cat. No. 03CH37439), (IEEE),*
525 3822–3825.

526 Xue, W., and Zaidi, A. (2021). Bayesian sensitivity analysis for missing data using the e-
527 value. *arXiv preprint arXiv:2108.13286*.